Structural Engineering and Mechanics, *Vol. 47, No. 4 (2013) 559-573*
DOI: http://dx.doi.org/10.12989/sem.2013.47.4.559

Axisymmetric large deflection analysis of fully and partially loaded shallow spherical shells

Murat Altekin* and Receb F. Yükseler[a]

Department of Civil Engineering, Yildiz Technical University, 34220, Esenler, Istanbul, Turkey

(Received March 31, 2013, Revised August 12, 2013, Accepted August 16, 2013)

Abstract. Geometrically non-linear axisymmetric bending of a shallow spherical shell with a clamped or a simply supported edge under axisymmetric load was investigated numerically. The partial load was introduced by the Heaviside step function, and the solution was obtained by the finite difference and the Newton-Raphson methods. The thickness of the shell was considered to be uniform and the material was assumed to be homogeneous and isotropic. Sensitivity analysis was made for three geometrical parameters. The accuracy of the algorithm was checked by comparing the central deflection, the radial membrane stress at the edge, or the transverse shear force with the solutions of plates and shells in the literature and good agreement was obtained. The main findings of the study can be outlined as follows: (i) If the shell is fully loaded the central deflection of a clamped shell is larger than that of a simply supported shell provided that the shell is not very shallow, (ii) if the shell is partially loaded the central deflection of the shell is sensitive to the parameters of thickness, depth, and partial loading but the influence of the boundary conditions is negligible.

Keywords: shell, non-linear, partial loading, bending, plate

1. Introduction

The studies on bending, buckling and dynamic analyses of rotational symmetric caps occupy great part in the excessive literature on shells (Sofiyev and Özyigit 2012). Linear theories have mostly been used in these studies while the number of papers dealing with non-linear analysis has been increasing (Hamed *et al*. 2010, Sofiyev *et al*. 2009, Arciniega and Reddy 2007, Dube *et al*. 2001). If the amplitude of motion is of the same order as the thickness of the shell, the small deflection theory is inadequate and the use of the non-linear theory of shells which takes into account the large deflection with higher order bending and stretching effects is required (Nath and Alwar 1978).

Plate and shell structures have been used in aerospace, aviation, shipbuilding, bridge construction, structural engineering and automotive industry. The behavior of these structures can be highly non-linear due to small thickness or due to changes of geometry and stresses which exceed the elastic limit of the material (Teng and Rotter 1989). Therefore, non-linear analysis is needed for more accurate prediction of the deformation behavior (Zhang and Kim 2006).

*Corresponding author, Associate Professor, E-mail: altekin@yildiz.edu.tr
[a]Retired

http://www.techno-press.org/?journal=sem&subpage=8 ISSN: 1225-4568 (Print), 1598-6217 (Online)

The analysis of shells dealing with geometric or constitutive non-linearity has been one of the leading research topics in solid mechanics, and is still the subject of investigation from experimental, theoretical or numerical points of view (Kim *et al*. 2010). This is partly because shells are widely used in many engineering applications (e.g., large-span roofs, storage silos, tanks, pressure vessels, underwater vehicles, nuclear reactors, ballistic missile bulkheads, offshore and space structures), and partly because in applied mechanics the large deflection of shells has been a challenging topic due to the complex coupled governing differential equations (Nath and Alwar 1978, Nath and Jain 1986). Since closed form solutions are only available for a limited number of cases depending on the theory, geometry, boundary conditions, material properties, and loading, the problem has been attacked by means of various numerical methods in the past two decades with the progress of computer technology. In the literature (Altekin and Yükseler 2012, Nie and Yao 2010, Maksimyuk *et al*. 2009, Filho and Awruch 2004, Sze *et al*. 2004, Hamdouni and Millet 2003, Ye 1991, Krayterman and Sabnis 1985, Nath *et al*. 1985, Pica *et al*. 1980, Perrone and Kao 1970) devoted to the non-linear analysis of shells and plates, uniform external pressure has received significant interest both due to its practical importance and due to its simplicity in formulation. Although the subject is one of the basic problems in structural mechanics, there is a scarcity of studies in which partially loaded shells have been investigated. Besides, as far as the authors know the influence of depth and thickness, and the effect of the size of the loaded portion of a shallow spherical shell undergoing large deflection have not yet been studied in detail.

The present study attempts to investigate the geometrically non-linear axisymmetric bending behavior of a shallow spherical thin shell with circular planform subject to partially applied axisymmetric pressure acting on a portion at the pole. The projection of this loaded region on the horizontal plane is a concentric circular area of radius b. A computationally efficient numerical solution was seeked to determine the displacements and the stress resultants. Sensitivity analysis was made to highlight the influence of the geometrical parameters (c, η, and μ) on the deflection and on the stress resultants. Central deflection response of a clamped and a simply supported shallow spherical shell was examined and the effect of the boundary conditions was clarified. The central deflection of a partially loaded shallow spherical shell was presented for future reference.

2. Formulation

By definition, a shell is a structural member with curved surfaces. Shells have all the characteristics of plates, along with an additional feature: curvature. Therefore, shells are sometimes referred to as curved plates. A shell is called ”thin” if $t/R \ll 1$ where $R = (a^2+h^2)/(2h)$, or for engineering accuracy a shell may be regarded as thin if the condition $\max(t/R) \leq 1/20$ is satisfied (Ventsel and Krauthammer 2001). For a large number of practical applications on thin shells, the aforementioned ratio lies in the range $1/1000 \leq t/R \leq 1/20$. A shell is called shallow if at any point of its middle surface the inequality $(\partial z/\partial r)^2 \ll 1$ holds. In case of a spherical shell z represents a paraboloid defined by $z = h(1-(r/a)^2)$, and a spherical shell is called ”shallow” if $\eta = h/(2a) < 1/8$ (Huang 1964, Akkas and Toroslu 1999).

2.1 Basic equations

First, due to the axisymmetry of both the loading and the geometry of the shell the partial differential shell equations are automatically transformed to ordinary differential equations. Next,

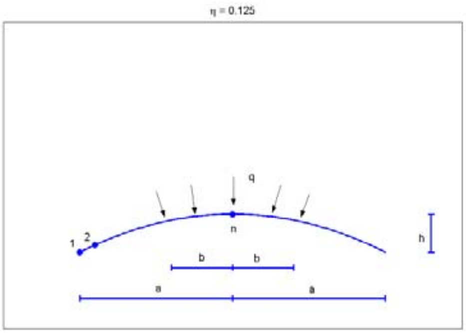

Fig. 1 Geometry of the shell, location of the grid points, and the loading

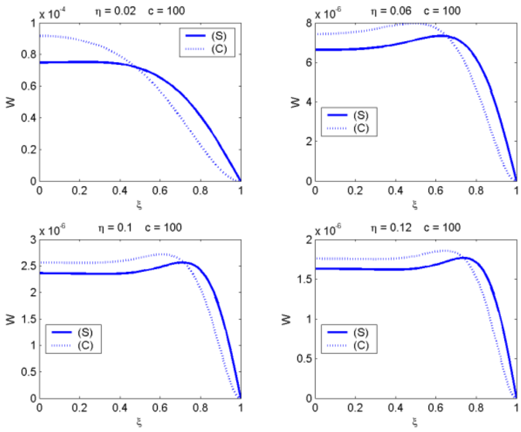

Fig. 2 Influence of η on W (c=100, μ=1)

the equilibrium equations, the stress-strain relations, and the strain-displacement relations presented by Huang (1964) are reorganized and rearranged in terms of three displacement components (w, u, β) where β = w', and three stress resultants (n_r, q_r, m_r) so as to make it possible to satisfy both the boundary conditions and the regularity conditions exactly. Therefore

$$L_1 = m_r + r\,m_r{}' + D\left(\frac{w'}{r} + \nu\,\beta'\right) - r\,q_r = 0 \tag{1}$$

$$L_2 = (1-\nu)n_r + r\,n_r{}' - E\,t\frac{u}{r} = 0 \tag{2}$$

$$L_3 = q_r + rq_r{}' + r\beta' n_r + 2h\frac{r}{a^2}(1+\nu)n_r + \frac{Et}{r}w'u + 2Et\frac{h}{a^2}u + \nu w' n_r + rHq = 0 \tag{3}$$

$$L_4 = m_r + D\,\beta' + D\frac{\nu}{r}\beta = 0 \tag{4}$$

$$L_5 = u' + 2\,h\frac{r}{a^2}\beta + \frac{1}{2}\beta^2 - \frac{\left(1-\nu^2\right)}{E\,t}n_r + \nu\frac{u}{r} = 0 \tag{5}$$

$$L_6 = w' - \beta = 0 \tag{6}$$

are obtained where $\mathrm{D} = \dfrac{\mathrm{Et}^3}{12\left(1-\nu^2\right)}$. The non-dimensional parameters are introduced by

$$W = \frac{w}{t}, \qquad U = \frac{u}{t}, \qquad c = \frac{a}{t}, \qquad Q = \frac{q}{E}, \tag{7}$$

$$N_r = \frac{n_r}{Et}, \qquad Q_r = \frac{q_r}{Et}, \qquad M_r = \frac{m_r}{Et^2}, \qquad \mu = \frac{b}{a} \tag{8}$$

$$\xi = \frac{r}{a}, \qquad \lambda = \frac{q\,a^4}{E\,t^4} = Q\,c^4, \qquad \alpha = \frac{\sigma_r^m\,a^2}{E\,t^2} = N_r\,c^2 \tag{9}$$

where $\sigma_r^m = n_r / t$ (Timoshenko and Woinowsky-Krieger 1959). Substituting the non-dimensional parameters defined in Eqs. (7)-(9) into Eqs. (1)-(6), the differential operators $(L_1, L_2, L_3, L_4, L_5, L_6)$ are obtained as follows:

$$L_1 = M_r + \xi \frac{dM_r}{d\xi} + \frac{1}{12\left(1-\nu^2\right)c^2\,\xi}\frac{dW}{d\xi} + \frac{\nu}{12\left(1-\nu^2\right)c}\frac{d\beta}{d\xi} - c\,\xi\,Q_r = 0 \tag{10}$$

$$L_2 = \left(1-\nu\right)N_r + \xi\frac{dN_r}{d\xi} - \frac{1}{c\,\xi}U = 0 \tag{11}$$

$$\begin{aligned} L_3 = {} & Q_r + \xi\frac{dQ_r}{d\xi} + \xi\frac{d\beta}{d\xi}N_r + 4\eta\left(1+\nu\right)\xi\,N_r + \frac{1}{c^2\,\xi}\frac{dW}{d\xi}U \\ & + 4\frac{\eta}{c}U + \frac{\nu}{c}\frac{dW}{d\xi}N_r + c\,\xi\,H\,Q = 0 \end{aligned} \tag{12}$$

$$L_4 = 12\left(1-\nu^2\right)c\,M_r + \frac{d\beta}{d\xi} + \frac{\nu}{\xi}\beta = 0 \tag{13}$$

$$L_5 = \frac{1}{c}\frac{dU}{d\xi} + 4\eta\,\xi\,\beta + \frac{1}{2}\beta^2 - \left(1-\nu^2\right)N_r + \frac{\nu}{c\,\xi}U = 0 \tag{14}$$

$$L_6 = \frac{1}{c}\frac{dW}{d\xi} - \beta = 0 \tag{15}$$

The loaded and the unloaded portions of the shell are defined by the Heaviside step function given by

$$H = H\left(\mu\right) = \begin{Bmatrix} 1, & if\;\; \mu - \xi \ge 0 \\ 0, & if\;\; \mu - \xi < 0 \end{Bmatrix}, \qquad 0 < \mu \le 1 \tag{16}$$

As a special case the solution of a fully loaded shallow spherical shell under uniform pressure is obtained for $\mu = 1$.

2.2 Boundary conditions and regularity conditions

The following boundary and regularity conditions are satisfied exactly:

- Boundary conditions along the clamped edge: at $\xi = 1$; $W = U = \beta = 0$
- Boundary conditions along the simply supported edge: at $\xi = 1$; $W = U = M_r = 0$
- Regularity conditions at the apex: at $\xi = 0$; $U = \beta = Q_r = 0$

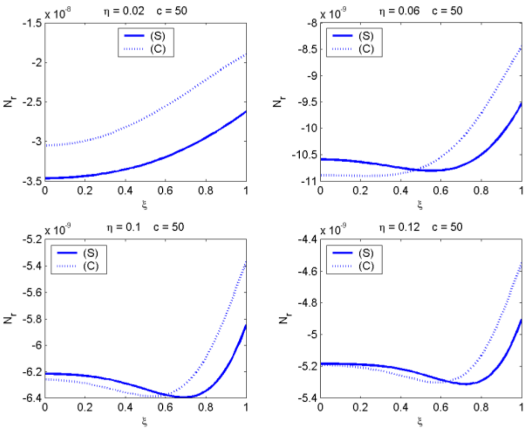

Fig. 3 Influence of η on N_r (c=50, μ=1)

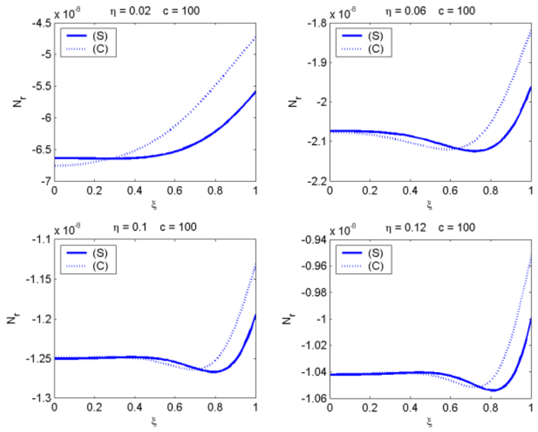

Fig. 4 Influence of η on N_r (c=100, μ=1)

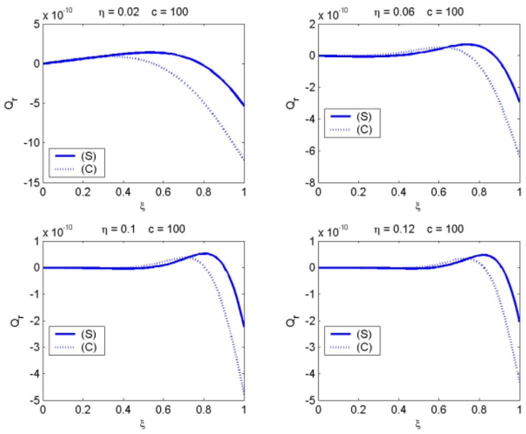

Fig. 5 Influence of η on Q_r (c=100, μ=1)

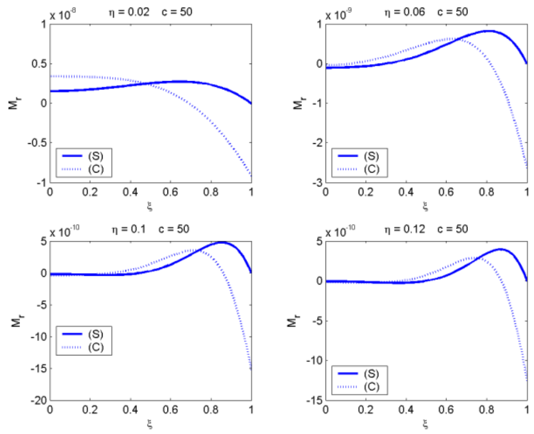

Fig. 6 Influence of η on M_r (c=50, μ=1)

3. Numerical results

Eqs. (10)-(15) were converted to algebraic equations via the forward, and backward finite difference formula. Six unknowns $\left(W, U, \beta, N_r, Q_r, M_r\right)$ were defined at each grid point where a grid point refers to a finite difference station located at ξ_i (Fig. 1). The algorithm was coded in C++. Numerical solutions were evaluated for clamped (C) and simply supported (S) shallow spherical shells of a = 1m. First, a fully loaded (i.e., μ = 1) shell under uniform pressure was examined (Tables 1-6, Figs. 2-13). Next, a partially loaded (i.e., μ ≠ 1) shell was investigated (Table 7, Figs. 14-26).

$$R_a = \frac{a^2}{2h}, \qquad K_a = \frac{1}{R_a}\frac{a^2}{t} = 4c\eta, \qquad \xi_i = \frac{n-i}{n-1}, \qquad i = 1, 2, ..., n \tag{17}$$

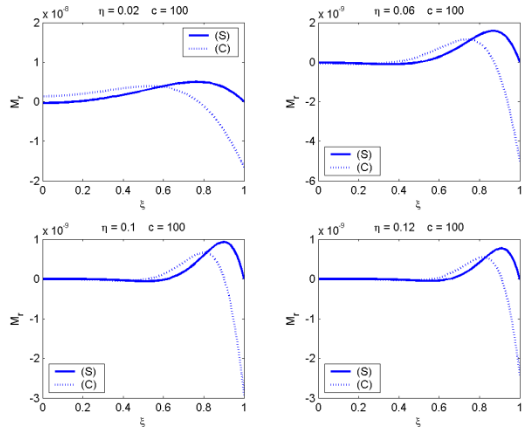

Fig. 7 Influence of η on M_r (c=100, μ=1)

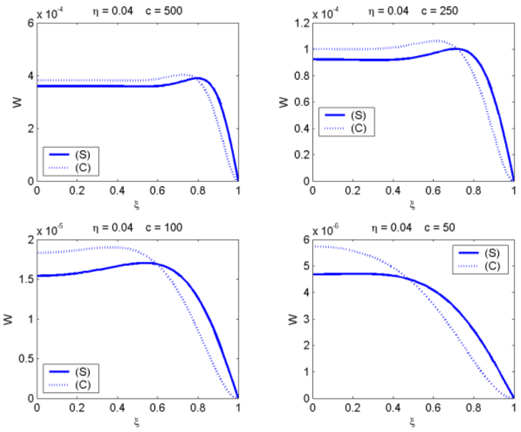

Fig. 8 Influence of c on W (μ=1)

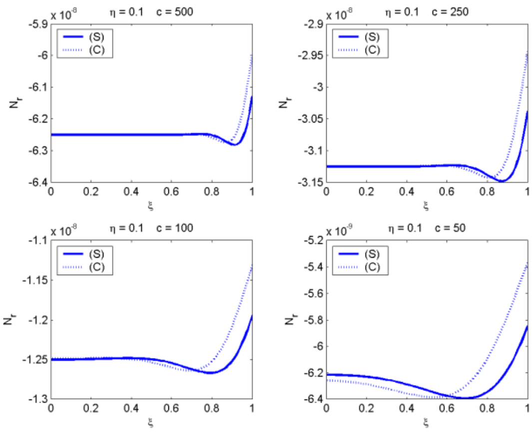

Fig. 9 Influence of c on N_r (η=0.10, μ=1)

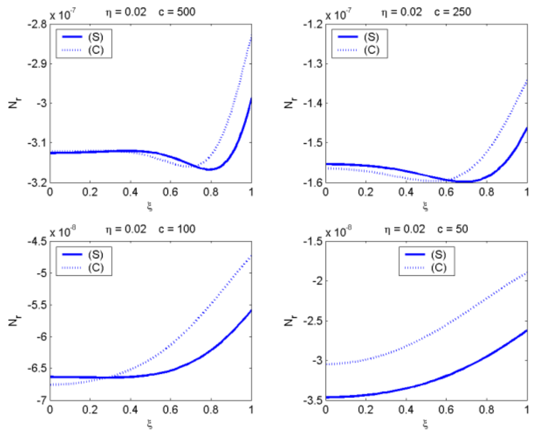

Fig. 10 Influence of c on N_r (η=0.02, μ=1)

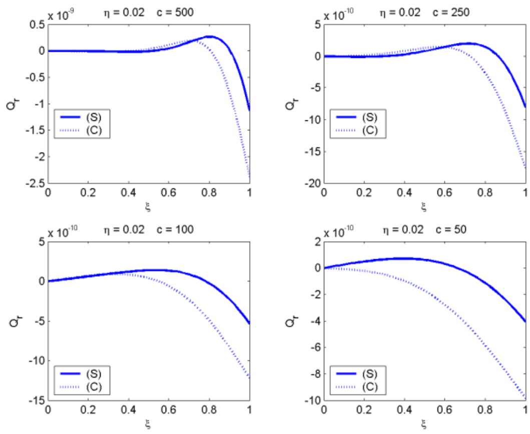

Fig. 11 Influence of c on Q_r (μ=1)

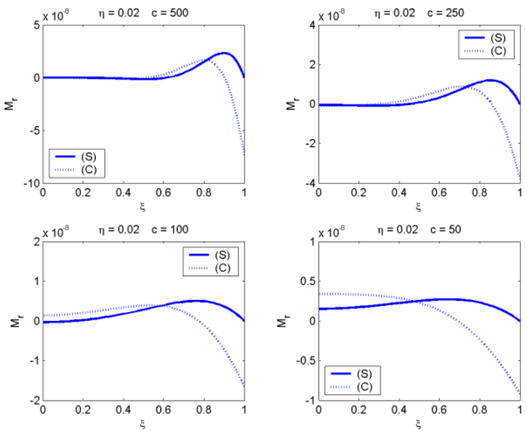

Fig. 12 Influence of c on M_r (η=0.02, μ=1)

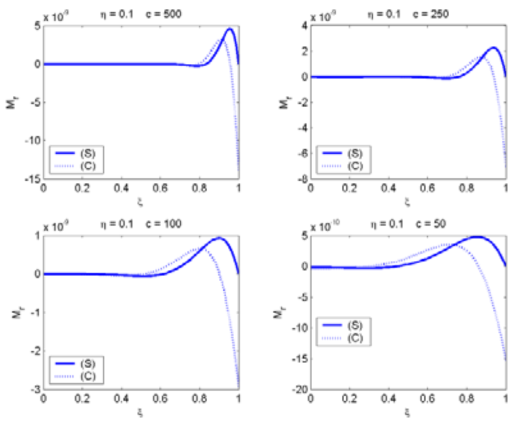

Fig. 13 Influence of c on M_r (η=0.10, μ=1)

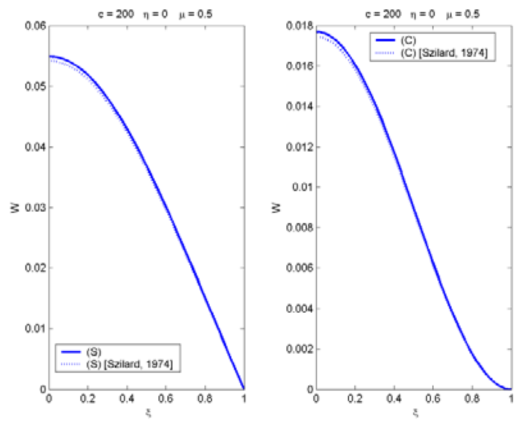

Fig. 14 W of a partially loaded plate (ν=0.3)

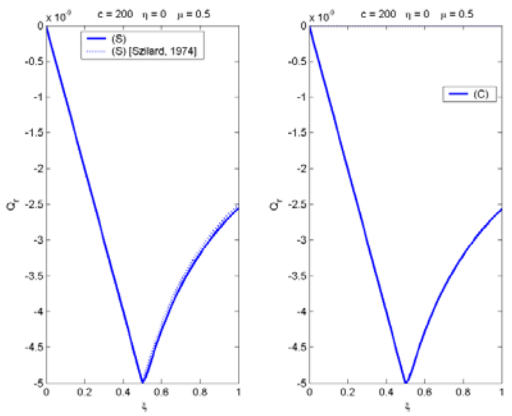

Fig. 15 Q_r of a partially loaded plate (ν=0.3)

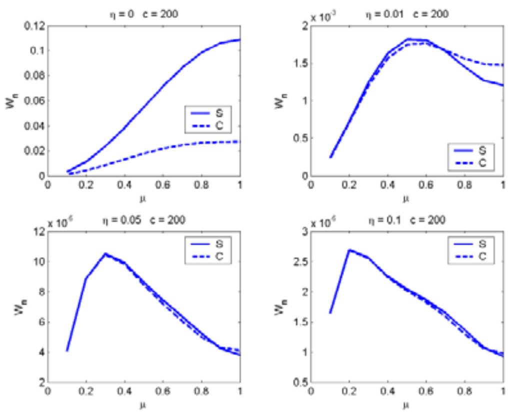

Fig. 16 Influence of μ and η on W_n (c=200, ν=0.3)

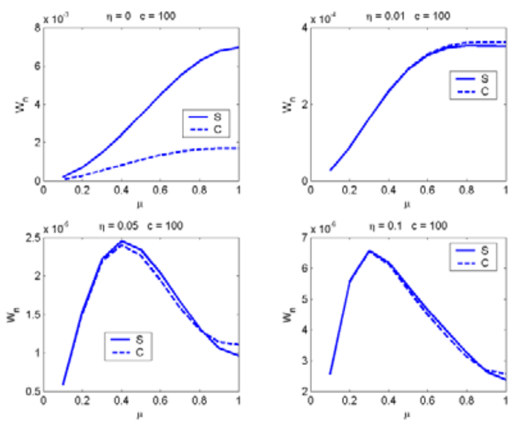

Fig. 17 Influence of μ and η on W_n (c=100, ν=0.3)

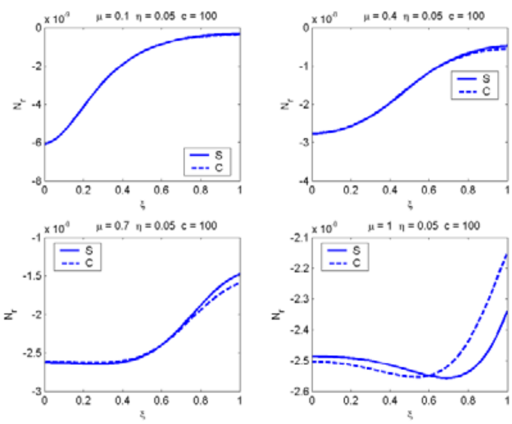

Fig. 18 Influence of μ on N_r (c=100, η= 0.05, ν=0.3)

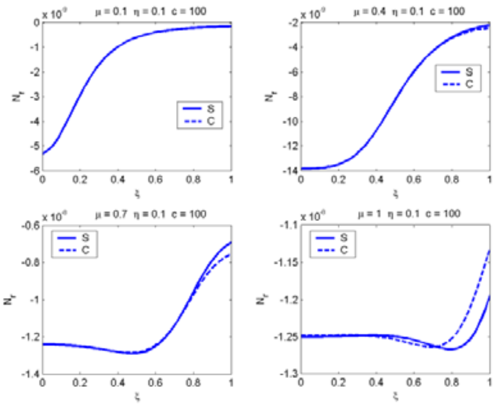

Fig. 19 Influence of μ on N_r (c=100, η =0.10, ν=0.3)

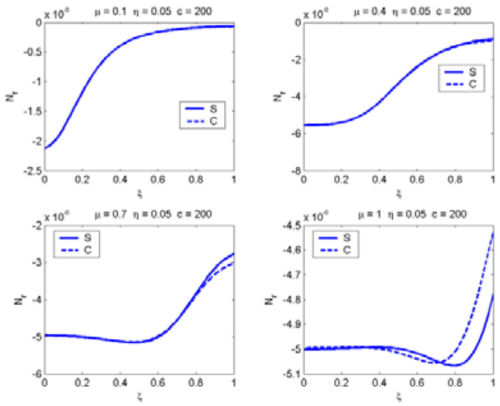

Fig. 20 Influence of μ on N_r (c=200, η =0.05, ν=0.3)

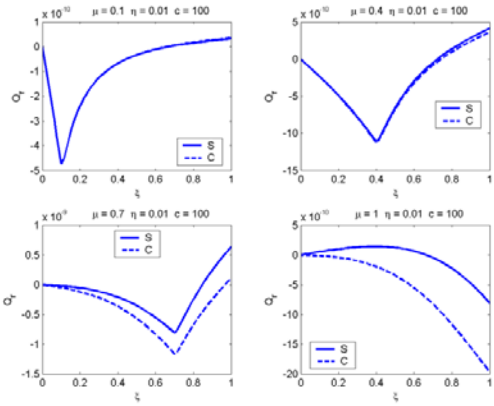

Fig. 21 Influence of μ on Q_r (c=100, η= 0.01, ν=0.3)

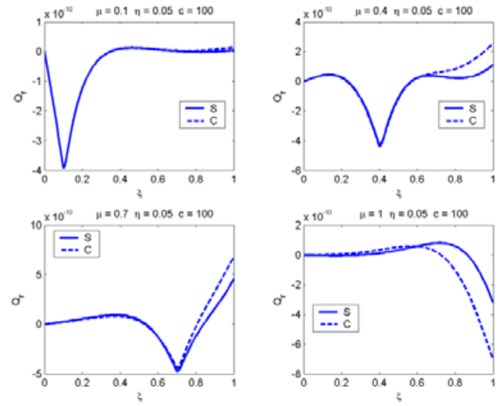

Fig. 22 Influence of μ on Q_r (c=100, η= 0.05, ν=0.3)

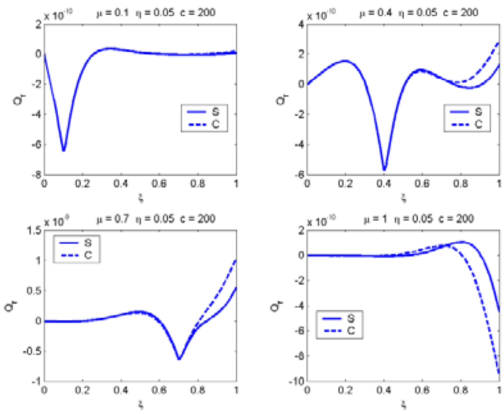

Fig. 23 Influence of μ on Q_r (c=200, η= 0.05, ν=0.3)

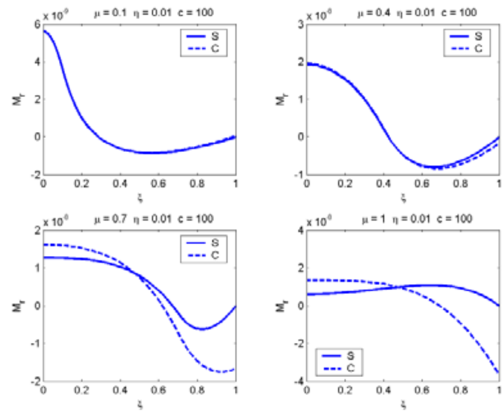

Fig. 24 Influence of μ on M_r (c=100, η= 0.01, ν=0.3)

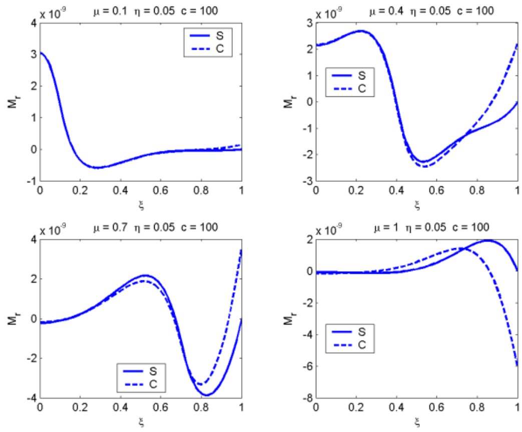

Fig. 25 Influence of μ on M_r (c=100, η=0.05, ν=0.3)

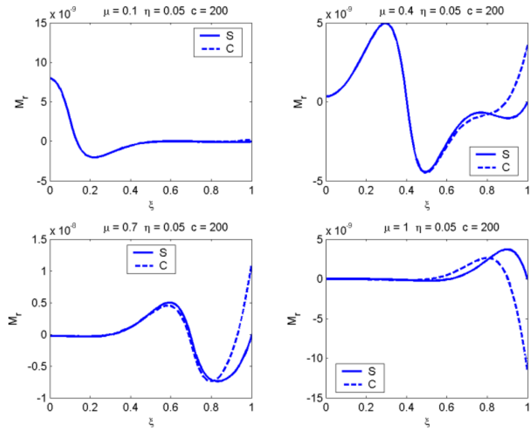

Fig. 26 Influence of μ on M_r (c=200, η=0.05, ν=0.3)

Table 1 Non-dimensional central deflection of a shallow spherical shell (C)

λ = 3	$K_a = 3$	$K_a = 4$	$K_a = 5$	$K_a = 6$	$K_a = 10$	$K_a = 20$
n = 51	0.2020	0.1199	0.0772	0.0528	0.0166	0.0033
n = 81	0.2019	0.1198	0.0771	0.0527	0.0166	0.0033
n = 101	0.2019	0.1198	0.0771	0.0527	0.0166	0.0033
λ = 5	$K_a = 3$	$K_a = 4$	$K_a = 5$	$K_a = 6$	$K_a = 10$	$K_a = 20$
n = 51	0.4027	0.2168	0.1344	0.0902	0.0278	0.0055
n = 81	0.4024	0.2166	0.1343	0.0901	0.0278	0.0055
n = 101	0.4024	0.2165	0.1343	0.0901	0.0278	0.0055

Table 2 Non-dimensional central deflection of a shallow spherical shell (S)

λ = 3	$K_a = 3$	$K_a = 4$	$K_a = 5$	$K_a = 6$	$K_a = 10$	$K_a = 20$
n = 51	0.2405	0.1155	0.0682	0.0444	0.0133	0.0029
n = 81	0.2405	0.1155	0.0682	0.0444	0.0133	0.0029
n = 101	0.2405	0.1155	0.0682	0.0444	0.0133	0.0029
λ = 5	$K_a = 3$	$K_a = 4$	$K_a = 5$	$K_a = 6$	$K_a = 10$	$K_a = 20$
n = 51	0.6285	0.2077	0.1170	0.0750	0.0221	0.0048
n = 81	0.6284	0.2077	0.1170	0.0750	0.0222	0.0048
n = 101	0.6284	0.2077	0.1170	0.0750	0.0222	0.0048

Table 3 Non-dimensional central deflection of a shallow spherical shell (C)

λ = 5	$K_a = 1$	$K_a = 2$	$K_a = 3$
n = 51	0.8601	0.8382	0.4027
n = 81	0.8609	0.8391	0.4024
n = 101	0.8612	0.8393	0.4024
(Nath and Alwar 1978)	0.853	0.852	0.375
(Nath *et al*. 1985)	0.862	0.840	0.402

Table 4 Non-dimensional central deflection of a shallow spherical shell (S)

	$\lambda = 10$	$\lambda = 1$	$\lambda = 3$
	$K_a = 1$	$K_a = 2$	$K_a = 3$
n = 51	1.9191	0.1605	0.2405
n = 81	1.9191	0.1605	0.2405
n = 101	1.9191	0.1605	0.2405
(Nath and Alwar 1978)	1.92	0.152	0.228
(Nath *et al*. 1985)	1.913	0.160	0.240

Table 5 Non-dimensional central deflection of a circular plate (C)

$\nu = 0.30$	$\lambda = 1$	$\lambda = 3$	$\lambda = 6$	$\lambda = 10$
n = 51	0.1678	0.4583	0.7694	1.0509
n = 81	0.1680	0.4586	0.7699	1.0515
n = 101	0.1680	0.4587	0.7700	1.0517
(Pica *et al*. 1980)	0.1682	0.4591	0.7702	1.0514
(Ye 1991)	0.1680	0.4588	0.7694	1.0512

Table 6 Non-dimensional central deflection and α of a circular plate (S)

$\nu = 0.25$	$\lambda = 3.07$	$\lambda = 3.07$	$\lambda = 7.18$	$\lambda = 7.18$	$\lambda = 25.66$	$\lambda = 25.66$
	W_n	α (Edge)	W_n	α (Edge)	W_n	α (Edge)
n = 51	0.8820	0.4687	1.2455	0.9669	1.9646	2.5448
n = 81	0.8820	0.4687	1.2455	0.9669	1.9646	2.5445
n = 101	0.8821	0.4687	1.2455	0.9669	1.9646	2.5445
(Ramachandra and Roy 2001)	0.884	0.478	1.247	0.984	1.966	2.595
(Federhofer and Egger 1946)*	0.882	0.469	1.245	0.967	1.965	2.544

Table 7 Influence of c, μ, and η on W_n (n = 81, $\nu = 0.3$)

	c = 100			c = 200		
η=0	μ = 0.4	μ = 0.7	μ = 1	μ = 0.4	μ = 0.7	μ = 1
(S)	0.0024	0.0055	0.0070	0.0385	0.0863	0.1088
(C)	0.0008	0.0015	0.0017	0.0131	0.0246	0.0273
η=0.01	μ = 0.4	μ = 0.7	μ = 1	μ = 0.4	μ = 0.7	μ = 1
(S)	$0.2339\text{x}10^{-3}$	$0.3474\ \text{x}10^{-3}$	$0.3517\ \text{x}10^{-3}$	0.0016	0.0017	0.0012
(C)	$0.2343\ \text{x}10^{-3}$	$0.3523\ \text{x}10^{-3}$	$0.3623\ \text{x}10^{-3}$	0.0016	0.0017	0.0015
η=0.05	μ = 0.4	μ = 0.7	μ = 1	μ = 0.4	μ = 0.7	μ = 1
(S)	$0.2453\ \text{x}10^{-4}$	$0.1666\ \text{x}10^{-4}$	$0.0965\ \text{x}10^{-4}$	$0.9889\ \text{x}10^{-4}$	$0.6322\ \text{x}10^{-4}$	$0.3786\ \text{x}10^{-4}$
(C)	$0.2400\ \text{x}10^{-4}$	$0.1582\ \text{x}10^{-4}$	$0.1106\ \text{x}10^{-4}$	$0.9787\ \text{x}10^{-4}$	$0.6017\ \text{x}10^{-4}$	$0.4107\ \text{x}10^{-4}$
η=0.10	μ = 0.4	μ = 0.7	μ = 1	μ = 0.4	μ = 0.7	μ = 1
(S)	$0.6180\ \text{x}10^{-5}$	$0.3951\ \text{x}10^{-5}$	$0.2366\ \text{x}10^{-5}$	$0.2245\ \text{x}10^{-4}$	$0.1640\ \text{x}10^{-4}$	$0.0924\ \text{x}10^{-4}$
(C)	$0.6117\ \text{x}10^{-5}$	$0.3761\ \text{x}10^{-5}$	$0.2567\ \text{x}10^{-5}$	$0.2228\ \text{x}10^{-4}$	$0.1582\ \text{x}10^{-4}$	$0.0981\ \text{x}10^{-4}$

* These results were taken from (Ramachandra and Roy, 2001), since the authors do not have access to (Federhofer and Egger, 1946).

3.1 Convergence studies and accuracy of the algorithm

The convergence studies, performed for Q = 1×10^{-6} and v = 0.3, revealed that n = 81 was sufficient for admissable accuracy (Tables 1-4). Circular plates of $t = 0.02$ m were examined by simply setting η = 0 (Tables 5-6). The central deflections of shells and plates, and the radial membrane stress to be developed at the edge of the plate computed in the current study agree well with those presented in the published studies of other researchers (Tables 3-6). Just for consistency with references (Nath and Alwar 1978, Nath *et al*. 1985), the geometry of the shell was characterized by λ and K_a. The non-linear bending solution of a partially loaded circular plate was also checked and good agreement was obtained (Figs. 14-15). The graphical representations of the deflection and the shear force cited as (Szilard 1974) depicted in Figs. 14-15 were plotted by using the formulae of Szilard (1974).

3.2 Influence of the geometrical parameters

The influence of the parameters was investigated by sensitivity analysis using the numerical parameters $50 \leq c \leq 1000$, and Q = 1×10^{-10} (Figs. 2-26, Table 7). The main findings of the study can be outlined as follows:

• If the shell is fully loaded the central deflection of a clamped shell is larger than that of a simply supported shell provided that $K_a \geq 4$ (Tables 1-2).

• W_n of a shallow spherical shell subject to fully applied uniform pressure can be estimated approximately by the relationship given by $W_n = Y\dfrac{\exp(-K_a/\lambda)}{\sqrt{K_a}}$ where Y is a scalar coefficient which may be determined by the method of least squares (Tables 1-2).

• In case of partial loading W_n is sensitive to c, η, and μ but the influence of the boundary conditions on W_n is negligible (Table 7).

• As the shell becomes deeper, the location of the grid point where W_{max} develops moves to the edge of the shell (Fig. 2).

• As the shell becomes deeper, N_r decreases, and the influence of the boundary conditions on N_r weakens (Figs. 3-4).

• As c increases, the influence of the boundary conditions on N_r weakens (Figs. 3-4).

• As η increases, the influence of the boundary conditions on Q_r and M_r becomes significant at the edge of the shell (Figs. 5-7).

• As η is raised, the magnitude of M_r developed at the pole decreases. As η or c is raised, the size of the circular area at the pole where constant M_r develops increases. The location of the grid point where the same M_r is produced by simply supported and clamped shells moves to the edge of the shell (Figs. 6-7).

• As c is decreased, W decreases non-linearly, and the location of the grid point where the same deflection develops for simply supported and clamped cases moves to the apex of the shell (Fig. 8).

• The influence of the boundary conditions on N_r is negligible if the shell is deep. However, N_r becomes more sensitive to the boundary conditions when η decreases (Figs. 9-10).

• As c is decreased, Q_r decreases at the support (Fig. 11).

• As c and η increase, the radius of the concentric circular region at the pole on which identical M_r develops for simply supported and clamped shells, increases. The influence of η on M_r is more

Table 8 Influence of the non-linearity on W_n and on the stress resultants ($n = 81$, $\nu = 0.3$)

	$c = 100$, $\mu = 0.5$	$c = 100$, $\mu = 1$	$c = 200$, $\mu = 0.5$	$c = 200$, $\mu = 1$	Parameter (Location)
$\eta = 0.01$ (S)	$W_n < 0.20$	$W_n < 0.20$	$W_n < 0.20$	$W_n < 0.18$	W_n (Center)
$\eta = 0.01$ (C)	$W_n < 0.20$	$W_n < 0.20$	$W_n < 0.20$	$W_n < 0.25$	
$\eta = 0.05$ (S)	$W_n < 0.21$	$W_n < 0.15$	$W_n < 0.63$	$W_n < 0.32$	
$\eta = 0.05$ (C)	$W_n < 0.20$	$W_n < 0.15$	$W_n < 0.60$	$W_n < 0.30$	
$\eta = 0.10$ (S)	$W_n < 0.62$	$W_n < 0.31$	$W_n < 0.50$	$W_n < 0.30$	
$\eta = 0.10$ (C)	$W_n < 0.61$	$W_n < 0.30$	$W_n < 0.50$	$W_n < 0.36$	
$\eta = 0.01$ (S)	$W_n < 0.25$	$W_n < 0.30$	$W_n < 0.30$	$W_n < 0.22$	N_r (Center)
$\eta = 0.01$ (C)	$W_n < 0.25$	$W_n < 0.22$	$W_n < 0.29$	$W_n < 0.35$	
$\eta = 0.05$ (S)	$W_n < 0.40$	$W_n < 0.18$	$W_n < 0.40$	$W_n < 0.32$	
$\eta = 0.05$ (C)	$W_n < 0.30$	$W_n < 0.15$	$W_n < 0.30$	$W_n < 0.30$	
$\eta = 0.10$ (S)	$W_n < 0.39$	$W_n < 0.33$	$W_n < 0.42$	$W_n < 0.30$	
$\eta = 0.10$ (C)	$W_n < 0.38$	$W_n < 0.35$	$W_n < 0.42$	$W_n < 0.37$	
$\eta = 0.01$ (S)	$W_n < 0.55$	$W_n < 0.20$	$W_n < 0.30$	$W_n < 0.15$	Q_r (Edge)
$\eta = 0.01$ (C)	$W_n < 0.30$	$W_n < 0.12$	$W_n < 0.30$	$W_n < 0.10$	
$\eta = 0.05$ (S)	$W_n < 0.20$	$W_n < 0.12$	$W_n < 0.30$	$W_n < 0.15$	
$\eta = 0.05$ (C)	$W_n < 0.20$	$W_n < 0.13$	$W_n < 0.24$	$W_n < 0.10$	
$\eta = 0.10$ (S)	$W_n < 0.30$	$W_n < 0.16$	$W_n < 0.59$	$W_n < 0.12$	
$\eta = 0.10$ (C)	$W_n < 0.30$	$W_n < 0.15$	$W_n < 0.40$	$W_n < 0.08$	
$\eta = 0.01$ (S)	$W_n < 0.30$	$W_n < 0.35$	$W_n < 0.30$	$W_n < 0.11$	M_r (Center)
$\eta = 0.01$ (C)	$W_n < 0.30$	$W_n < 0.30$	$W_n < 0.29$	$W_n < 0.34$	
$\eta = 0.05$ (S)	$W_n < 0.35$	$W_n < 0.10$	$W_n < 0.19$	$W_n < 0.15$	
$\eta = 0.05$ (C)	$W_n < 0.32$	$W_n < 0.08$	$W_n < 0.15$	$W_n < 0.08$	
$\eta = 0.10$ (S)	$W_n < 0.18$	$W_n < 0.15$	$W_n < 0.18$	$W_n < 0.09$	
$\eta = 0.10$ (C)	$W_n < 0.18$	$W_n < 0.06$	$W_n < 0.19$	$W_n < 0.19$	

dominant than that of c. Furthermore, M_r is not sensitive to the boundary conditons of the shell at the pole close to the apex (Figs. 12-13).

• As the depth is raised, W_n decreases, and the maximum central deflection develops for smaller μ. A clamped shell deflects larger than a simply supported shell at the apex for the higher values of μ (e.g., $\mu > 0.8$). As c increases, the maximum central deflection develops for smaller μ (Figs. 16-17).

• As μ increases, the location of the grid point where $\max(N_r)$ develops moves to the edge of the shell. The boundary conditions do not have any significant effect on N_r. As the depth increases, N_r decreases. As c increases, N_r increases. The influence of the boundary conditions on N_r at the pole is negligible (Figs. 18-20).

• As μ is raised, the influence of the boundary conditions on Q_r becomes stronger when the radial coordinate increases. The Q_r vs ξ curve has the form of a "V", and the curve has a steep descent and a steep ascent at $\xi = \mu$. Thickness of the shell does not change the trend of the Q_r vs ξ curve. As c increases, the magnitude of Q_r increases. When the shell is partially loaded (i.e., $\mu < 1$), the influence of the boundary conditions on Q_r can be considered to be negligible (Figs. 21-23).

• As μ or η is raised, the value of M_r at the apex decreases. When the shell is fully loaded, increase in c results in increase of the size of the circular area at the pole where constant M_r develops (Figs. 24-26).

3.3 Influence of the non-linearity

The influence of the non-linearity on the deflection and on the stress resultants was examined for a number of different values of Q, and the interval in which the influence of the geometrical non-linearity can be neglected was shown in terms of W_n (Table 8).

• The results reveal that the influence of the geometrical non-linearity depends on both the size of the loaded region and the geometrical parameters (c and η) of the shell (Table 8). However, if $W_n < 0.15$, the aforementioned effect is negligible for deflection.

• $W_n < 0.10$ can be considered to be the region for which the aforementioned effect is negligible for the internal forces (N_r, Q_r, M_r).

• As the depth of the shell decreases the influence of the boundary conditions on the effect of non-linearity becomes negligible.

4. Conclusions

A simply supported plate deflects larger than a clamped plate does, but this statement does not always hold for shallow spherical shells. Although from geometrical aspects, plates are special cases of shells, the bending response of shallow spherical shells is quite different from that of plates if the perimeter of the shell is simply supported or clamped.

The size of the surface on which the load acts at the pole of the shell is found to be crucial in investigating the influence of the boundary conditions on the stress resultants. It can also be stated that there is a strong relationship between the depth of the shell and the stress resultants.

The main advantage of the current formulation is that there is only one coupled and one non-linear equation including only the first derivatives of the parameters among six differential operators. Rapid convergence was obtained with less computational effort. Furthermore, not only uniform pressure, but also any type of axisymmetric load can easily be treated without requiring large computational storage. The procedure is well suited for axisymmetric non-linear analysis of shallow spherical shells and circular plates.

References

Akkas, N. and Toroslu, R. (1999), “Snap-through buckling analyses of composite shallow spherical shells”, *Mechanics of Composite Materials and Structures*, **6**(4), 319-330.

Altekin, M. and Yükseler, R.F. (2012), ”Axisymmetric large deflection analysis of an annular circular plate subject to rotational symmetric loading”, *Proceedings of the Eleventh Int. Conference on Computational Structures Technology*, Dubrovnik, September.

Arciniega, R.A. and Reddy, J.N. (2007), “Large deformation analysis of functionally graded shells”, *Int. J. of Solids and Structures*, **44**(6), 2036-2052.

Dube, G.P., Joshi, S. and Dumir, P.C. (2001), “Nonlinear analysis of thick shallow spherical and conical orthotropic caps using Galerkin’s method”, *Applied Mathematical Modelling*, **25**(9), 755-773.

Filho, L.A.D. and Awruch, A.M. (2004), “Geometrically nonlinear static and dynamic analysis of shells and plates using the eight-node hexahedral element with one-point quadrature”, *Finite Elements in Analysis*

and Design, **40**(11), 1297-1315.
Federhofer, K. and Egger, H. (1946), "Berechnung der dunnen kreisplatte mit grosser ausbiegung", *Akad. Wiss. Wien. Math.-Naturwiss*, **155**(2a), 15-43.
Hamdouni, A. and Millet, O. (2003), "Classification of thin shell models deduced from the nonlinear three-dimensional elasticity. part I: the shallow shells", *Archives of Mechanics*, **55**(2), 135-175.
Hamed, E., Bradford, M.A. and Gilbert, R.I. (2010), "Nonlinear long-term behavior of spherical shallow thin-walled concrete shells of revolution", *Int. J. of Solids and Structures*, **47**(2), 204-215.
Huang, N.C. (1964), "Unsymmetrical buckling of thin shallow spherical shells", *J. of Applied Mechanics*, **31**(3), 447-457.
Krayterman, B. and Sabnis, G.M. (1985), "Large deflected plates and shells with loading history", *J. of Engineering Mechanics*, **111**(5), 653-663.
Kim, T.H., Park, J.G., Choi, J.H. and Shin, H.M. (2010), "Nonlinear dynamic analysis of reinforced concrete shell structures", *Structural Engineering and Mechanics*, **34**(6), 685-702.
Maksimyuk, V.A., Storozhuk, E.A. and Chernyshenko, I.S. (2009), "Using mesh-based methods to solve nonlinear problems of statics for thin shells", *Int. Applied Mechanics*, **45**(1), 32-56.
Nath, Y. and Alwar, R.S. (1978), "Non-linear static and dynamic response of spherical shells", *Int. J. of Non-Linear Mechanics*, **13** (3), 157-170.
Nath, Y., Dumir, P.C. and Bhatia, R.S. (1985), "Non-linear static and dynamic analysis of circular plates and shallow spherical shells using the collocation method", *Int. J. for Numerical Methods in Engineering*, **21**(3), 565-578.
Nath, Y. and Jain, R.K. (1986), "Non-linear studies of orthotropic shallow spherical shells on elastic foundation", *Int. J. of Non-Linear Mechanics*, **21**(6), 447-458.
Nie, G.H. and Yao, J.C. (2010), "An asymptotic solution for non-linear behavior of ımperfect shallow spherical shells", *J. of Mechanics*, **26**(2), 113-122.
Perrone, N. and Kao, R. (1970), "Large deflection response and buckling of partially and fully loaded spherical caps", *AIAA J.*, **8**(12), 2130-2136.
Pica, A., Wood, R.D. and Hinton, E. (1980), "Finite element analysis of geometrically nonlinear plate behaviour using a Mindlin formulation", *Computers and Structures*, **11**(3), 203-215.
Ramachandra, L.S. and Roy, D. (2001), "A novel technique in the solution of axisymmetric large deflection analysis of a circular plate", *J. of Applied Mechanics*, **68**(5), 814-816.
Sofiyev, A.H., Omurtag, M.H. and Schnack, E. (2009), "The vibration and stability of orthotropic conical shells with non-homogeneous material properties under a hydrostatic pressure", *J. of Sound and Vibration*, **319** (3-5), 963-983.
Sofiyev, A. and Özyigit, P. (2012), "Thermal buckling analysis of non-homogeneous shallow spherical shells", *J. of the Faculty of Engineering and Architecture of Gazi University*, **27**(2), 397-405. (in Turkish)
Sze, K.Y., Liu, X.H. and Lo, S.H. (2004), "Popular benchmark problems for geometric nonlinear analysis of shells", *Finite Elements in Analysis and Design*, **40**(11), 1551-1569.
Szilard, R. (1974), *Theory and Analysis of Plates*, Prentice-Hall, Englewood Cliffs, New Jersey, USA.
Teng, J.G. and Rotter, J.M. (1989), "Elastic-plastic large deflection analysis of axisymmetric shells", *Computers and Structures*, **31**(2), 211-233.
Timoshenko, S.P. and Woinowsky-Krieger, S. (1959), *Theory of Plates and Shells*, McGraw-Hill Int. Editions, Singapore.
Ventsel, E. and Krauthammer, T. (2001), *Thin Plates and Shells: Theory, Analysis, and Applications*, Marcel Dekker Inc., USA.
Ye, J. (1991), "Large deflection analysis of axisymmetric circular plates with variable thickness by the boundary element method", *Applied Mathematical Modelling*, **15**(6), 325-328.
Zhang, Y.X. and Kim, K.S. (2006), "Geometrically nonlinear analysis of laminated composite plates by two new displacement-based quadrilateral plate elements", *Composite Structures*, **72**(3), 301-310.

Nomenclature

D, E, R	flexural rigidity, Young's modulus, radius of the shell
H, Q, U, W	Heaviside step function, non-dimensional uniform pressure, non-dimensional horizontal radial displacement, non-dimensional deflection
K_a, R_a, W_n	non-dimensional approximate curvature, approximate radius, non-dimensional central deflection
L_i, M_r, N_r, Q_r	i^{th} differential operator (i = 1, 2, …, 6), non-dimensional meridional moment per unit length of the shell, non-dimensional membrane force, non-dimensional transverse shear force
a, c, t, z	base radius (or half span) of the shell, parameter of thickness, thickness of the shell, equation of the middle surface of the shell
b, h, n, q	base radius of the circular loaded portion at the pole, rise of the apex, total number of grid points located along the meridian on the middle surface of the shell, uniform pressure
r, u, w	radial coordinate, horizontal radial displacement, deflection
m_r, n_r, q_r	meridional moment per unit length of the shell, membrane force, transverse shear force
α, β, η	parameter of radial membrane stress, rotation, parameter of depth
λ, μ, ν, ξ	parameter of load, parameter of partial loading, Poisson's ratio, non-dimensional radial coordinate
σ_r^m, ξ_i	radial membrane stress, non-dimensional radial coordinate of the i^{th} grid point
$(\ )'$	differentiation with respect to r